ADVANCED MATERIALS

Supporting Information

for *Adv. Mater.*, DOI: 10.1002/adma.201101917

Using Magnetic Levitation for Three Dimensional Self-Assembly

*Katherine A. Mirica , Filip Ilievski , Audrey K. Ellerbee , Sergey S. Shevkoplyas , and George M. Whitesides **

Using Magnetic Levitation for Three Dimensional Self-Assembly

SUPPORTING INFORMATION

Katherine A. Mirica[1], Filip Ilievski[1], Audrey K. Ellerbee[1], Sergey S. Shevkoplyas[3], and George M. Whitesides[1,2]*

[1] Department of Chemistry and Chemical Biology, Harvard University

12 Oxford St., Cambridge, MA 02138

[2] Wyss Institute for Biologically Inspired Engineering, Harvard University

3 Blackfan Circle, Boston, MA 02115

[3] Department of Biomedical Engineering, Tulane University,

500 L. Boggs Building, New Orleans, LA 70118

* Corresponding author: George M. Whitesides (gwhitesides@gmwgroup.harvard.edu)

General Materials and Methods. The NdFeB magnets (square prisms: grade N50, 2 in × 2 in × 1 in, Model # NB063-N50; rectangular prisms: grade N42, 4 in × 2 in × 1 in, Model# NB079) were purchased from Applied Magnets (www.magnet4less.com) and positioned with like poles facing each other within an aluminum casing. The aluminum casing for the magnets was designed and fabricated by Gaudreau Engineering (West Warwick, RI) for a fee. All chemicals were purchased from Sigma-Aldrich (Atlanta, GA) and used without further purification, unless noted otherwise. All plastics, polymeric sheets, and tapes were purchased from McMaster-Carr (Princeton, NJ; www.mcmaster.com), unless noted otherwise. Sheets of polymethylmethacrylate (PMMA) were purchased from Astra Products (Baldwin, NY; www.astraproducts.com). Sheets of polystyrene were purchased from Utrecht (Cambridge, MA; www.utrechtart.com). Polyvinyl chloride tape (PVC) and aluminum tape were purchased from McMaster-Carr (Princeton, NJ; www.mcmaster.com). Scotch® Double-Sided Carpet Tape (CT 2010) was purchased from 3M. Mirrored mylar tape was purchased from The Band Hall (Nashville, TN; www.thebandhall.com). Masking and labeling tapes were purchased from VWR International. We purchased a plastic Fresnel lens from Edmund Industrial Optics (Barrington, NJ), and a convex lens from Thorlabs (Newton, NJ; www.thorlabs.com). Plastic diffraction gratings and a red laser pointer were purchased from Edmund Scientifics (Tonawanda, NY; www.scientificsonline.com). We used a 100 mW green laser purchased from Wicked Lasers (www.wickedlasers.com) for demonstrating the function of levitating optical components.

Figure S1. Photograph of the device for MagLev. The device comprises two NdFeB magnets positioned with like poles facing each other within an aluminum casing.

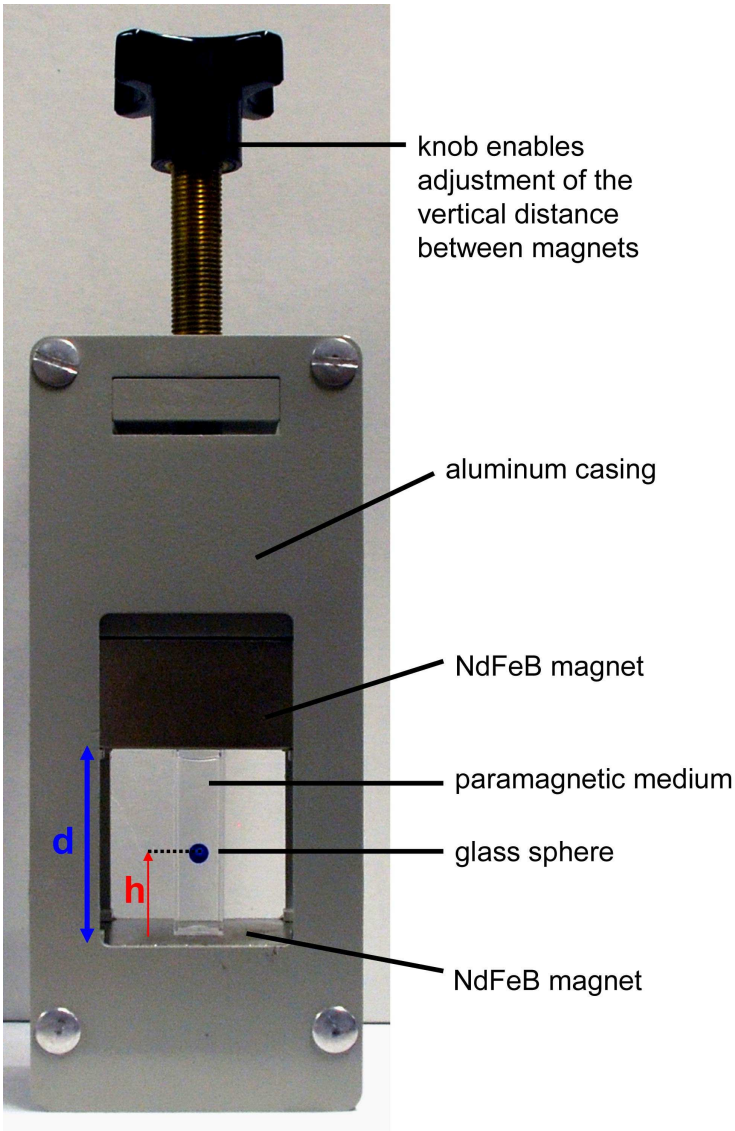

Figure S2. A) Simulation of the magnetic field in the YZ-plane at d = 25, 35, and 45 mm. The magnitude of the magnetic field in these simulations is constrained between 0 T and 0.4 T. Dotted square circumscribes the region occupied by levitating objects in panels B and C. B) Photographs of three squares (10 × 10 mm) fabricated from layers of PMMA and PVC levitating in 1.5 M $MnCl_2$. The density defines the vertical levitation height of each square, and the gradient of the magnetic field in the Z-direction (controlled by varying d) determines the vertical spacing between the squares. C) Photographs of a square with an asymmetric density pattern made from PS and PVC levitating in 1.0 M $MnCl_2$ at d = 25, 35, and 45 mm. Varying the value of d alters the tilt angle of the square with respect to the gravitational axis.

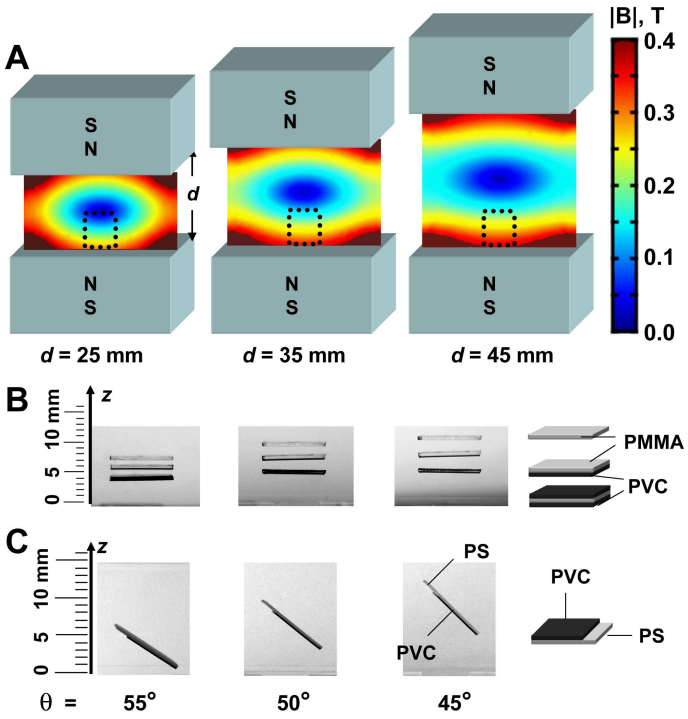

Figure S3. Photographs of self-assembly inside a closed container. A) A mirror and a pinhole sink to the bottom of the container in the absence of an applied magnetic field. B) Positioning the container between the two magnets causes assembly of the components. C) The levitating mirror guides light through the pinhole.

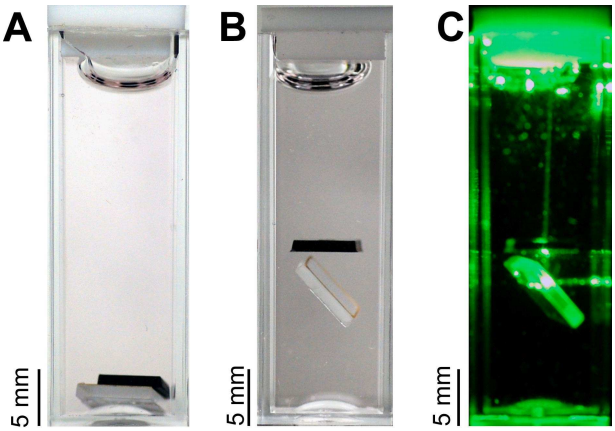

Figure S4. Photographs illustrating the use of tilting for controlling the orientation of levitating mirrors. Photographs show two tilted mirrors and a red filter placed in between them for reference. A) Initial position of levitating objects introduced into the MagLev device. B) Tilting the device to the left rotates the mirrors with the heaviest part pointing towards the direction of tilt. C) Re-leveling the device traps the mirrors with the heaviest part pointing left. D) Tilting the device to the right rotates the mirrors with the heaviest part pointing right. E) Re-leveling the device traps the mirrors with the heaviest part pointing right.

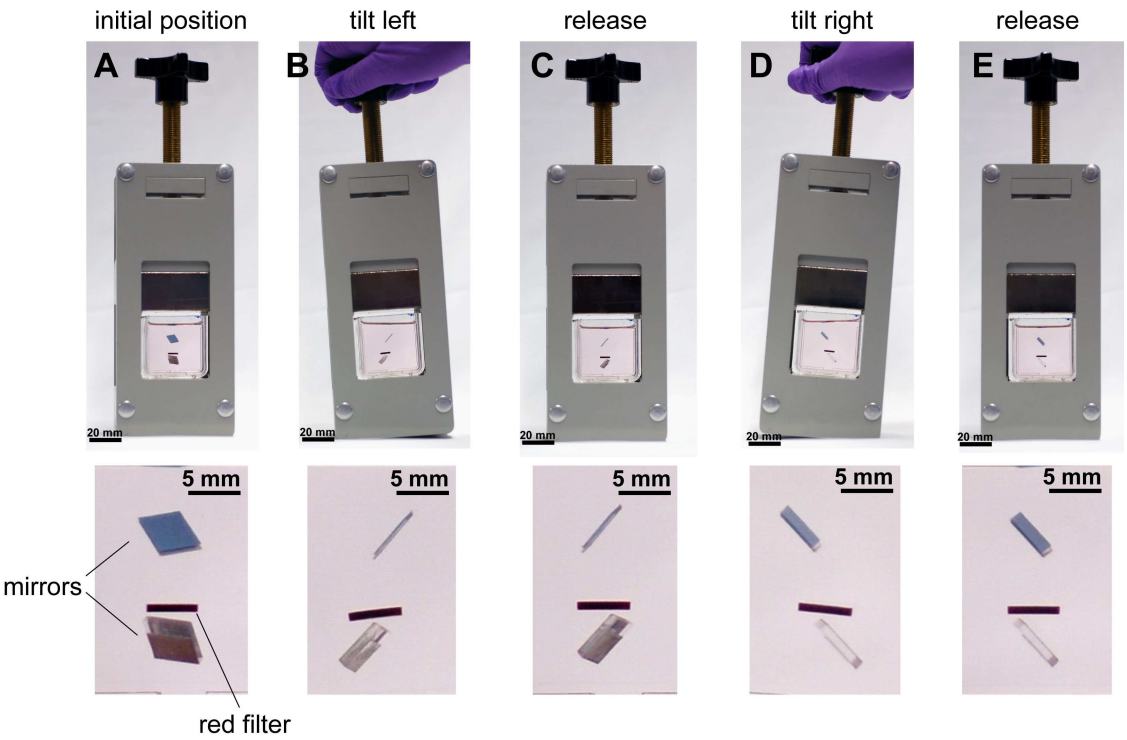

Figure S5. A) Photographs demonstrating alignment and positioning of mirrors levitating in aqueous 1.5 M $MnCl_2$. Levitating mirrors guide the laser beam by reflection; the distance between the magnets (*d*) controls the tilt angle of each mirror. B) A levitating mirror guides light through a convex lens (left) and a Fresnel lens (right). C) A levitating mirror suspended in aq. 1.5 M $MnCl_2$ guides light through a transmissive diffraction grating. The grating produces a diffraction pattern on the bottom of the container. Scale bars in all photographs are 5 mm.

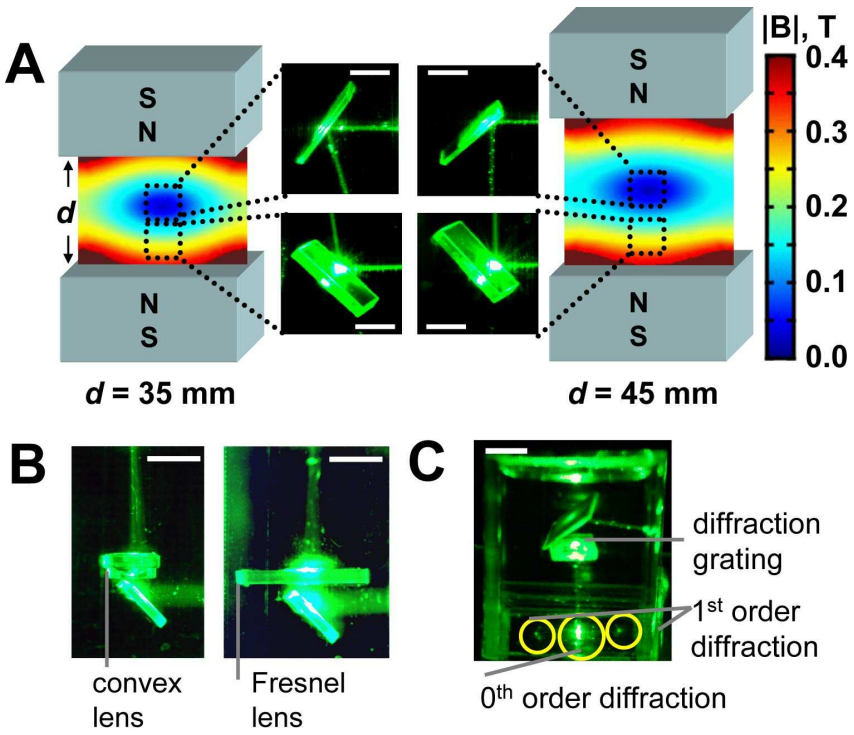

Fabrication of Components from Layers of Polystyrene (PS) and Polyvinyl Chloride (PVC) Tape. To fabricate the components shown in Figure 2B (main text), we pressed the PVC tape against the surface of polystyrene and manually cut this polymer composite using scissors into squares of 10 mm × 10 mm. To fabricate the components shown in Figure 2C, we cut polystyrene into squares with dimensions of 10 mm × 10 mm, and PVC tape into squares with dimensions of 8 × 10 mm using scissors. We then pressed PVC against one surface of polystyrene to fabricate the components shown in Figure 2C (left), and against both surfaces for component shown in Figure 2C (right).

Fabrication of Components from Layers of Polymethylmethacrylate (PMMA) and Polyvinyl Chloride (PVC) Tape. Components shown in Figure 3 were fabricated from layers of PMMA and PVC and cut into specific shapes using a laser cutter (VersaLASER, Model VLS 3.5, Universal Laser Systems) using a general procedure shown in Figure 2A. The component levitating at the top was made from red-colored PMMA (Figure 3) having a thickness of 1 mm. The component levitating in the middle was made from a sheet of PMMA (0.5 mm thick) sandwiched between two layers of orange-colored PVC tape. The component levitating at the bottom was made from a sheet of PMMA (0.2 mm thick) sandwiched between three layers (one on top, and two on the bottom) of blue-colored PVC tape.

Fabrication of Components with Optical Function.

Lenses, Filters, and Pinholes. A plastic Fresnel lens (Aspheric Fresnel Lens, 0.6" X 0.6", 0.2" FL, part number NT43-021) was purchased from Edmund Industrial Optics

(Barrington, NJ; www.edmundoptics.com), and plastic convex lens (part # CAY046) was purchased from Thorlabs (Newton, NJ; www.thorlabs.com); these lenses were levitated without further modification. Red and green filters were fabricated from red- and green-colored PMMA (1 mm thickness, Astra Products, www.astraproducts.com) by laser-cutting the PMMA sheet into circles with a diameter of 7 mm each. A PMMA-based IR filter was supplied by Astra Products, and cut into a 7-mm diameter circle using a laser cutter. The pinhole was fabricated from PMMA-based IR filter (0.5 mm thickness, Astra Products, www.astraproducts.com) by laser-cutting the PMMA sheet into a square with dimensions of 6 mm × 6 mm having a 0.5 mm hole at the center.

Mirrors. To fabricate the mirror shown in Figure 4A (top) we pressed mirrored mylar tape (The Band Hall, Nashville, TN) against the surface of PMMA having a thickness of 0.2 mm, and used a laser cutter to cut a square of 7 mm × 7 mm. We then covered the non-reflective surface of this object with two layers of masking tape with dimensions of 6 mm × 7 mm. To fabricate the mirror shown in Figure 4A (bottom) we pressed mirrored mylar tape against the surface of PMMA having a thickness of 1.0 mm, and used a laser cutter to cut a square of 7 mm × 7 mm. We then covered the non-reflective surface of this object with one layer of aluminum tape with dimensions of 5 mm × 7 mm. The mirrors shown in Figure 4B were fabricated using an analogous process.

Diffraction Gratings. We used squares of PMMA (7 mm × 7 mm with a 4 mm × 4 mm cutout window in the center) as supports for commercial plastic diffraction gratings (Edmund Scientific's, Tonawanda, NY). To fabricate the diffraction grating, we covered

the surface of PMMA (0.5 mm thick) with double-sided adhesive tape and cut the square using a laser cutter. We then pressed the commercial plastic diffraction grating against the adhesive tape. The orientation of the lines of the diffraction grating with respect to the supporting PMMA square can be used to control the diffraction pattern when multiple gratings on square supports are aligned on top of one another by MagLev.

Fabrication of Interlocking Components. The interlocking structures were generated by placing components with programmed shape and density (see details below) into a plastic container filled with 1.8 M $MnCl_2$ and positioning the container in the MagLev device. The container was equipped on its side with a hole and tubing for draining the fluid. The fluid was removed manually using a syringe.

Concentric Circles. To fabricate the concentric circles shown in Figure 6, we adhered various kinds of tapes to a PMMA sheet with a thickness of 1 mm, and cut the shapes out using the laser cutter. We used the following adhesive tapes: two layers of blue labeling tape (VWR International) for the first shape, none for the second shape (just red PMMA), a layer of orange PVC tape on one side and a layer of white Bytac® film (VWR International) on the other side for the third shape, a layer of blue PVC tape on one side and a layer of white polytetrafluoroethylene (PTFE) film with adhesive backing (0.005'' in thickness, McMaster Carr) on the other side for the fourth shape. To fabricate the base we used a laser cutter to engrave a pattern that would collect the concentric circles on top of it, and cut it using a laser cutter. The base was fabricated from PMMA (1.5 mm thickness) adhered to two layers of PTFE film with adhesive backing (0.005'' thickness).

Interlocking Squares. The red component was fabricated from red PMMA (1 mm in thickness, Astra Products) by laser cutting. Yellow, green, and blue components were fabricated from colored PMMA (3 mm in thickness, McMaster Carr) by laser cutting and engraving. The levitation height of each component was programmed by layering adhesive tape/film onto the surface of PMMA prior to laser cutting. We used two layers of yellow labeling tape (VWR International) for the yellow component, one layer of PTFE film (0.005'' thickness) with adhesive backing for the blue component, and two layers of the same PTFE film for the green component.

Derivation of an Analytical Expression for the Angle of Tilt.

For a diamagnetic object with a homogeneous distribution of density and magnetic susceptibility throughout its volume and that is suspended in a paramagnetic solution under an applied magnetic field, $\vec{B}$ (T), eqn (1) gives the magnetic force, $\vec{F}_m$ (N), and eqn (2) gives the force of gravity, $\vec{F}_g$ (N), acting on the object.

$$\vec{F}_m = \frac{(\chi - \chi_m)}{\mu_0} V \left(\vec{B} \cdot \vec{\nabla}\right) \vec{B} \tag{1}$$

$$\vec{F}_g = (\rho - \rho_m) V \vec{g} \tag{2}$$

In these equations, χ_m (unitless) is the magnetic susceptibility of the paramagnetic medium and χ (unitless) is the magnetic susceptibility of the suspended object, $\mu_0 = 4\pi \times 10^{-7}$ (N·A^{-2}) is the magnetic permeability of free space, V (m^3) is the

volume of the object, ρ (kg·m^{-3}) is the density of the object, ρ_m (kg·m^{-3}) is the density of the medium, and $\vec{g}$ is the vector of gravity.

The force of gravity (corrected for the effect of buoyancy), $\vec{F}_g$, is always directed to or away from the center of the Earth, and the magnitude of this force does not depend on the position of the object inside the vessel as long as the densities of the paramagnetic medium and the object remain constant for the duration of the levitation experiment. The magnetic force acting on the diamagnetic object, $\vec{F}_m$, is directed towards the minimum of the magnetic field, $\vec{B}$, and the magnitude of this force depends on the position of object in the field. In a 3D Cartesian coordinate system in which the Z-axis is aligned with the direction of the vector of gravity, $\vec{g} = (0, \quad 0, \quad -g)$, the magnetic and gravitational forces acting on the homogeneous diamagnetic object are given by eqns (3) and (4).

$$\vec{F}_g = (\rho - \rho_m) V \vec{g} = \begin{pmatrix} 0 \\ 0 \\ -(\rho - \rho_m) V g \end{pmatrix} \tag{3}$$

$$\vec{F}_m = \frac{(\chi - \chi_m)}{\mu_0} V \left(\vec{B} \cdot \vec{\nabla} \right) \vec{B} = \begin{pmatrix} \frac{(\chi - \chi_m)}{\mu_0} V \left(B_x \frac{\partial B_x}{\partial x} + B_y \frac{\partial B_x}{\partial y} + B_z \frac{\partial B_x}{\partial z} \right) \\ \frac{(\chi - \chi_m)}{\mu_0} V \left(B_x \frac{\partial B_y}{\partial x} + B_y \frac{\partial B_y}{\partial y} + B_z \frac{\partial B_y}{\partial z} \right) \\ \frac{(\chi - \chi_m)}{\mu_0} V \left(B_x \frac{\partial B_z}{\partial x} + B_y \frac{\partial B_z}{\partial y} + B_z \frac{\partial B_z}{\partial z} \right) \end{pmatrix} \tag{4}$$

For a composite object (subscript *c*) of heterogeneous density comprising two non-overlapping components (subscripts *a* and *b*) of homogeneous densities whose centers of mass are connect by a massless rod of length *L*, the total force acting on the composite is a vector sum of the forces acting on its constituent objects, eqn (5).

$$
\begin{aligned}
&\vec{F}_c = \vec{F}_{ga} + \vec{F}_{gb} + \vec{F}_{ma} + \vec{F}_{mb} = \\
&= (\rho_a - \rho_m) V_a \vec{g} + (\rho_b - \rho_m) V_b \vec{g} + \\
&+ \frac{(\chi_a - \chi_m)}{\mu_0} V_a \left(\vec{B}(\vec{r}_a) \cdot \vec{\nabla} \right) \vec{B}(\vec{r}_a) + \frac{(\chi_b - \chi_m)}{\mu_0} V_b \left(\vec{B}(\vec{r}_b) \cdot \vec{\nabla} \right) \vec{B}(\vec{r}_b)
\end{aligned}
\tag{5}
$$

In eqn (5), $\vec{r}_a$ is the coordinate of the center of mass of one component, and $\vec{r}_b$ is the coordinate of the center of mass of the other component. (Note that for an object with a homogeneous distribution of density over its volume, the center of mass and the center of volume coincide.) The vector form of the net force acting on the composite object is then given by eqn (6), in which the expressions involving the magnetic field for each of the two components are evaluated at the location of the components.

$$
\vec{F}_c = \begin{pmatrix}
\frac{(\chi_a - \chi_m) V_a}{\mu_0} \left(B_x \frac{\partial B_x}{\partial x} + B_y \frac{\partial B_x}{\partial y} + B_z \frac{\partial B_x}{\partial z} \right)_a + \frac{(\chi_b - \chi_m) V_b}{\mu_0} \left(B_x \frac{\partial B_x}{\partial x} + B_y \frac{\partial B_x}{\partial y} + B_z \frac{\partial B_x}{\partial z} \right)_b \\
\frac{(\chi_a - \chi_m) V_a}{\mu_0} \left(B_x \frac{\partial B_y}{\partial x} + B_y \frac{\partial B_y}{\partial y} + B_z \frac{\partial B_y}{\partial z} \right)_a + \frac{(\chi_b - \chi_m) V_b}{\mu_0} \left(B_x \frac{\partial B_y}{\partial x} + B_y \frac{\partial B_y}{\partial y} + B_z \frac{\partial B_y}{\partial z} \right)_b \\
-(\rho_a - \rho_m) V_a g - (\rho_b - \rho_m) V_b g + \frac{(\chi_a - \chi_m) V_a}{\mu_0} \left(B_x \frac{\partial B_z}{\partial x} + B_y \frac{\partial B_z}{\partial y} + B_z \frac{\partial B_z}{\partial z} \right)_a + \\
+ \frac{(\chi_b - \chi_m) V_b}{\mu_0} \left(B_x \frac{\partial B_z}{\partial x} + B_y \frac{\partial B_z}{\partial y} + B_z \frac{\partial B_z}{\partial z} \right)_b
\end{pmatrix}
\tag{6}
$$

Equation (6) can be simplified if we assume that the magnetic susceptibilities of the two components of the composite object are the same ($\chi_a = \chi_b = \chi_c$) and take into account the geometrical configuration of the experimental setup we used for magnetic levitation. The exact analytical expression describing the magnetic field between two identical rectangular permanent magnets in an anti-Helmholtz configuration in 3D is

fairly complex. A 3D numerical simulation (COMSOL Multiphysics, COMSOL, Inc., Burlington, MA) of the magnetic field in our magnetic levitation setup (two identical NdFeB, 5 cm × 5 cm × 2.5 cm, permanent magnets positioned with like poles facing each other and separated by a distance d = 45mm) reveals that within an approximately 10-mm radius of the centerline connecting the centers of the two magnets,

$$B_x \frac{\partial B_x}{\partial x} >> \left(B_y \frac{\partial B_x}{\partial y} + B_z \frac{\partial B_x}{\partial z} \right),\ B_y \frac{\partial B_y}{\partial y} >> \left(B_x \frac{\partial B_y}{\partial x} + B_z \frac{\partial B_y}{\partial z} \right), \text{ and}$$

$$B_z \frac{\partial B_z}{\partial z} >> \left(B_x \frac{\partial B_z}{\partial x} + B_y \frac{\partial B_z}{\partial y} \right).$$

We assume that the composite object levitates within the 10-mm radius around the centerline. Eqn (6) can then be simplified using the results of these computations and the assumption regarding the magnetic susceptibilities of the components to yield eqn (7).

$$\vec{F}_c = \begin{pmatrix} \frac{(\chi_c - \chi_m)}{\mu_0} \left(V_a \left(B_x \frac{\partial B_x}{\partial x} \right)_a + V_b \left(B_x \frac{\partial B_x}{\partial x} \right)_b \right) \\ \frac{(\chi_c - \chi_m)}{\mu_0} \left(V_a \left(B_y \frac{\partial B_y}{\partial y} \right)_a + V_b \left(B_y \frac{\partial B_y}{\partial y} \right)_b \right) \\ -(\rho_a - \rho_m) V_a g - (\rho_b - \rho_m) V_b g + \frac{(\chi_c - \chi_m)}{\mu_0} \left(V_a \left(B_z \frac{\partial B_z}{\partial z} \right)_a + V_b \left(B_z \frac{\partial B_z}{\partial z} \right)_b \right) \end{pmatrix}$$

(7)

We set the system of coordinates such that the Z-axis coincides with the centerline (the line connecting the centers of the two magnets), the origin is in the center of the top surface of the bottom magnet, and the YZ plane contains the centers of mass of both components of the composite object. In this coordinate system, $B_x(y,z) = 0$ in the YZ plane, and therefore any translation and rotation of the composite object approaching the equilibrium will localize in the YZ plane.

Our numerical simulation also shows that within about a 10-mm radius of the centerline, $B_y(y,z)$ varies virtually linearly in Y-direction ($B_y = 0$ for $y = 0$), and $B_z(y,z)$ varies virtually linearly in Z-direction ($B_z = 0$ for $z = \frac{d}{2}$). If we neglect the small variation of $B_y(y,z)$ in the Z-direction and of $B_z(y,z)$ in the Y-direction, these components of the magnetic field can then be approximated with expressions given by eqns (8) and (9).

$$B_y(y,z) = \alpha_y y \tag{8}$$

$$B_z(y,z) = \alpha_z\left(z - \frac{d}{2}\right) \tag{9}$$

Equation (7) for the net force acting on the composite object can then be simplified to yield eqn (10).

$$\vec{F}_c = \begin{pmatrix} 0 \\ \frac{(\chi_c - \chi_m)}{\mu_0}\left(V_a\alpha_y^2 y_a + V_b\alpha_y^2 y_b\right) \\ -(\rho_a - \rho_m)V_a g - (\rho_b - \rho_m)V_b g + \frac{(\chi_c - \chi_m)}{\mu_0}\left(V_a\alpha_z^2\left(z_a - \frac{d}{2}\right) + V_b\alpha_z^2\left(z_b - \frac{d}{2}\right)\right) \end{pmatrix} \tag{10}$$

For a composite object levitating at equilibrium, the net force acting on the object and the torque around any pivot point must equal zero. The first condition of equilibrium yields eqn (11).

$$\begin{pmatrix} 0 \\ \frac{(\chi_c - \chi_m)}{\mu_0}\left(V_a \alpha_y^2 y_a + V_b \alpha_y^2 y_b\right) \\ -(\rho_a - \rho_m)V_a g - (\rho_b - \rho_m)V_b g + \frac{(\chi_c - \chi_m)}{\mu_0}\left(V_a \alpha_z^2 \left(z_a - \frac{d}{2}\right) + V_b \alpha_z^2 \left(z_b - \frac{d}{2}\right)\right) \end{pmatrix} = \begin{pmatrix} 0 \\ 0 \\ 0 \end{pmatrix} \tag{11}$$

The second condition written for a pivot point located at the center of mass of component *b* gives eqn (12), in which $\vec{r} = \vec{r}_a - \vec{r}_b$.

$$\vec{r} \times \left(\vec{F}_{ga} + \vec{F}_{ma}\right) = \begin{pmatrix} x_a - x_b \\ y_a - y_b \\ z_a - z_b \end{pmatrix} \times \begin{pmatrix} 0 \\ \frac{(\chi_c - \chi_m)}{\mu_0} V_a \alpha_y^2 y_a \\ -(\rho_a - \rho_m)V_a g + \frac{(\chi_c - \chi_m)}{\mu_0} V_a \alpha_z^2 \left(z_a - \frac{d}{2}\right) \end{pmatrix} = \begin{pmatrix} 0 \\ 0 \\ 0 \end{pmatrix} \tag{12}$$

We can express the coordinates of the center of mass of component *b* through the coordinates of the center of mass of component *a* as is shown in eqn (13), in which θ is the angle of tilt of the composite object in YZ plane, defined as the angle between the Z-axis (vertical direction) and the link connecting the centers of mass of the two components comprising the object.

$$\begin{aligned} y_b &= y_a - L\sin\theta \\ z_b &= z_a - L\cos\theta \end{aligned} \tag{13}$$

Substituting eqn (13) into eqn (11) and eqn (12) and performing the vector multiplication yields eqns (14). By solving the system of equations given in eqn (14), we obtain eqns (15).

$$\begin{cases} \dfrac{(\chi_c-\chi_m)}{\mu_0}\left(V_a\alpha_y^2 y_a + V_b\alpha_y^2\left(y_a - L\sin\theta\right)\right)=0 \\ -(\rho_a-\rho_m)V_a g-(\rho_b-\rho_m)V_b g+\dfrac{(\chi_c-\chi_m)}{\mu_0}\left(V_a\alpha_z^2\left(z_a-\dfrac{d}{2}\right)+V_b\alpha_z^2\left(z_a-L\cos\theta-\dfrac{d}{2}\right)\right)=0 \\ \left(-(\rho_a-\rho_m)V_a g+\dfrac{(\chi_c-\chi_m)}{\mu_0}V_a\alpha_z^2\left(z_a-\dfrac{d}{2}\right)\right)L\sin\theta-\dfrac{(\chi_c-\chi_m)}{\mu_0}V_a\alpha_y^2 y_a L\cos\theta=0 \end{cases}$$

(14)

$$\begin{cases} y_a=\dfrac{V_b}{V_a+V_b}L\sin\theta \\ z_a=\dfrac{d}{2}+\dfrac{(\rho_a V_a-\rho_m V_a+\rho_b V_b-\rho_m V_b)g\mu_0}{\alpha_z^2(\chi_c-\chi_m)(V_a+V_b)}+\dfrac{V_b}{V_a+V_b}L\cos\theta \\ \cos\theta=\dfrac{(\rho_b-\rho_a)g\mu_0}{(\chi_c-\chi_m)(\alpha_y^2-\alpha_z^2)L} \end{cases} \tag{15}$$

Combining eqn (13) with eqn (15) yields eqn (16).

$$\begin{cases} y_a=\dfrac{V_b}{V_a+V_b}L\sin\theta \\ z_a=\dfrac{d}{2}+\dfrac{(\rho_a V_a-\rho_m V_a+\rho_b V_b-\rho_m V_b)g\mu_0}{\alpha_z^2(\chi_c-\chi_m)(V_a+V_b)}+\dfrac{V_b}{V_a+V_b}L\cos\theta \\ y_b=-\dfrac{V_a}{V_a+V_b}L\sin\theta \\ z_b=\dfrac{d}{2}+\dfrac{(\rho_a V_a-\rho_m V_a+\rho_b V_b-\rho_m V_b)g\mu_0}{\alpha_z^2(\chi_c-\chi_m)(V_a+V_b)}-\dfrac{V_a}{V_a+V_b}L\cos\theta \\ \cos\theta=\dfrac{(\rho_b-\rho_a)g\mu_0}{(\chi_c-\chi_m)(\alpha_y^2-\alpha_z^2)L} \end{cases} \tag{16}$$

From eqn (16) we find that, for a composite object near equilibrium, the angle of tilt is given by eqn (17), and the distance between the top surface of the bottom magnet

and the center of volume of the object (h , levitation height) is given by eqn (18), in which $\rho_c = \frac{\rho_a V_a + \rho_b V_b}{(V_a + V_b)}$ is the average density of the composite object.

$$\theta = \cos^{-1} \frac{(\rho_b - \rho_a) g \mu_0}{(\chi_c - \chi_m)(\alpha_y^2 - \alpha_z^2) L} \tag{17}$$

$$h = \frac{z_a V_a + z_b V_b}{V_a + V_b} = \frac{d}{2} + \frac{(\rho_c - \rho_m) g \mu_0}{\alpha_z^2 (\chi_c - \chi_m)} \tag{18}$$